Isochoric pVT and Phase Equilibrium Measurements for Carbon Dioxide + Nitrogen

Horacio A. Duarte-Garza,[†] James C. Holste, and Kenneth R. Hall*

Department of Chemical Engineering, Texas A&M University, College Station, Texas 77843

Kenneth N. Marsh and Bruce E. Gammon

Thermodynamics Researh Center, Texas A&M University, College Station, Texas 77843

We have designed and constructed an isochoric apparatus for fast and accurate pressure–volume–temperature (pVT) and phase equilibrium measurements. The apparatus allows isochoric (p, T at constant V) measurements for noncorrosive fluids over a wide range of pressures (7–105 MPa) and temperatures (100–450 K). Densities can be derived from densities determined at one isotherm (p, V at constant T) with another apparatus, such as a pycnometer or a Burnett apparatus. Temperatures are accurate to ±10 mK and precise to ±1 mK on ITS-90. Pressure measurements are accurate to ±10 kPa and precise to ±2 kPa. This apparatus requires about 20 min for temperature equilibration for measurements 2 K apart and about 50 min for measurements 10 K apart. We have measured 23 phase boundary points for three mole fractions, x_1 = 0.3991, 0.4459, and 0.5037, for CO_2 (1) + N_2 (2) at temperatures from 207 to 268 K and pressures from 10.8 to 21.5 MPa. The estimated accuracy is ±40 mK in temperature and ±17 kPa in pressure. The isochoric measurements used to obtain these phase boundary points extend from 205 to 300 K and from 8 to 80 MPa. We have determined the saturation density for 20 of the phase boundary points. The saturation densities and the densities along the isochores were derived from density measurements at 300 and 285 K measured with a pycnometer estimated to be accurate to ±0.1%. The behavior of the solid + fluid phase boundary is discussed.

Introduction

Among the most important thermodynamic information for fluids are pVT and phase equilibrium properties. Accurate volumetric data enable calculation of energy functions and estimation of transport properties. Phase equilibrium results are used in the design of most separation processes. Equations of state (EOS) can be tested directly against accurate density measurements, and comparison of phase equilibrium calculations against phase equilibrium measurements is a stringent test for an EOS because these calculations involve first derivatives of the EOS with respect to composition.

Phase equilibria and pVT values can be measured simultaneously in an isochoric experiment. The density for each isochore can be determined either by measuring the cell volume and the amount of charge or by measuring the density at one temperature using another apparatus (1, 2). Phase behavior is measured by observing the discontinuous change in the slope of an isochore which occurs at the phase boundary. A disadvantage of this experiment is the large number of measurements required to locate the phase boundary (at least four points along a given isochore).

In this paper, we report the design and construction of a high-pressure isochoric apparatus that significantly reduces the amount of time required to measure phase equilibria in an isochoric experiment. The apparatus measures p, T (isochores) of noncorrosive fluids over a wide range of pressures (7 ≤ p/MPa ≤ 105) and temperatures (100 ≤ T/K ≤ 450). The measured temperatures are accurate to ±10 mK and precise to ±1 mK with respect to ITS-90. The measured pressures are accurate to ±10 kPa

[†] Current address: Department of Chemical and Natural Gas Engineering, Texas A&M University–Kingsville, Kingsville, TX 78363.

and precise to ±2 kPa. The temperature of the sample cell can be controlled to ±2 mK, and equilibration takes about 50 min for points 10 K apart (3).

We present phase equilibria, isochoric densities, and isothermal densities for three CO_2 + N_2 mixtures at temperatures from 205 to 300 K and pressures from 8 to 80 MPa.

Experimental Section

Pressures and temperatures of phase boundaries were determined for three CO_2 + N_2 mixtures using a high-pressure isochoric apparatus, and the saturated densities were determined by coupling isochoric measurements to isothermal density measurements made with a pycnometer. A detailed description of the isochoric apparatus is part of this paper. A detailed description of the pycnometer has appeared elsewhere (4), and only a brief description is presented here. A description of the sample preparation is presented at the end of this section.

The apparatus, which consists of a high-pressure cell, pressure and temperature sensors, an isothermal shield, a vacuum chamber, a heating system, a cooling system, a vacuum system, a feed manifold, and a data acquisition and computer control system, has been designed to provide rapid and precise p, T measurements. The mass of the apparatus is minimized to allow rapid changes in temperature, and it is constructed of materials with high thermal conductivities to provide rapid thermal equilibration.

The cell is constructed from a Be–Cu alloy (Brush Wellman, Inc., alloy 3HT). This alloy has a combination of moderate tensile strength (750 MPa) and high thermal conductivity (250 W·m^{-1}·K^{-1} at 293 K). The temperature of the cell is measured with a platinum resistance thermometer, and the pressure is measured by a quartz
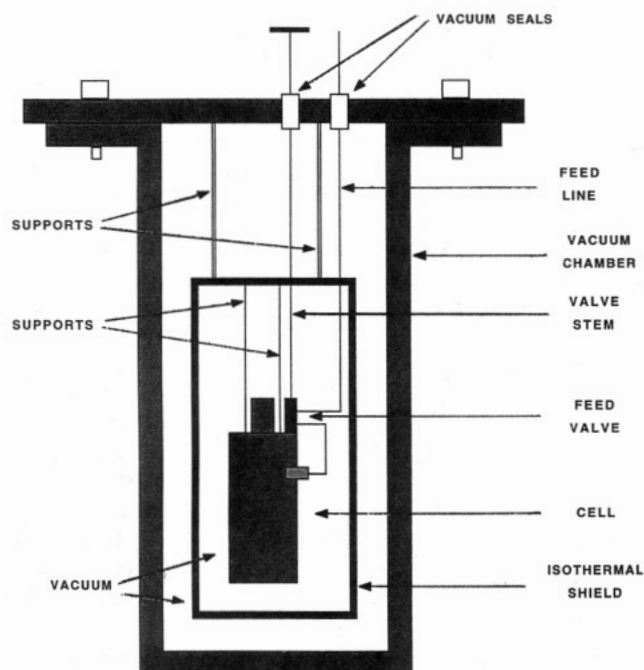
Figure 1. Vacuum chamber–isothermal shield–cell arrangement. Reflux tube, cooling coils, *etc.* are not shown in this figure; see Figure 3.

Figure 2. Schematic of the high-pressure cell.

pressure transducer placed inside the cell. This transducer limits the range of the apparatus to a maximum pressure of 105 MPa and a maximum temperature of 450 K. Temperature gradients are determined with multijunction thermopiles strategically placed about the cell.

The cell is surrounded by an isothermal shield situated inside a vacuum chamber. The isothermal shield minimizes heat exchange between the cell and its surroundings while the vacuum minimizes energy transfer between the cell and the isothermal shield and between the shield and the surroundings. The temperature of the isothermal shield is maintained 1–5 K lower than the temperature of the cell to create a small heat leak and facilitate the temperature control of the cell.

The vacuum chamber and the isothermal shield are nominal 6 in. (15 cm) and 4 in. (10 cm), respectively, aluminum pipe (schedule 40). The isothermal shield is suspended from the top plate of the vacuum chamber by four stainless steel tubes (0.635 cm o.d. and 0.254 mm wall thickness). The cell is suspended from the top plate of the isothermal shield by five stainless steel rods (0.317 cm o.d.). With this configuration, heat exchange by conduction through the supports is very small. Figure 1 is a schematic diagram of the apparatus.

The heating system consists of the following elements: a digital to analog converter, four heaters, four variable dc power supplies, four ac transformers, and four relay switches. A 32 Ω heater is wound around the isothermal shield, and a 30 Ω heater is wound around the cell. A 2 Ω heater is attached to the top plate, and another 2 Ω heater is attached to the bottom plate of the isothermal shield. A 25 W dc power supply is used for the isothermal shield heater, and three 4 W dc power supplies are used for the other heaters. The outputs of these dc power supplies are controlled with a digital computer while the ac settings are fixed and used in an on/off mode. The ac power provides fast heating, and the dc power provides control. The relays permit switching from ac to dc power and *vice versa*.

The feed manifold consists of a variable volume cell (a hand pump), a high-pressure Bourdon gauge, and a set of high-pressure valves. The feed manifold connects the cell
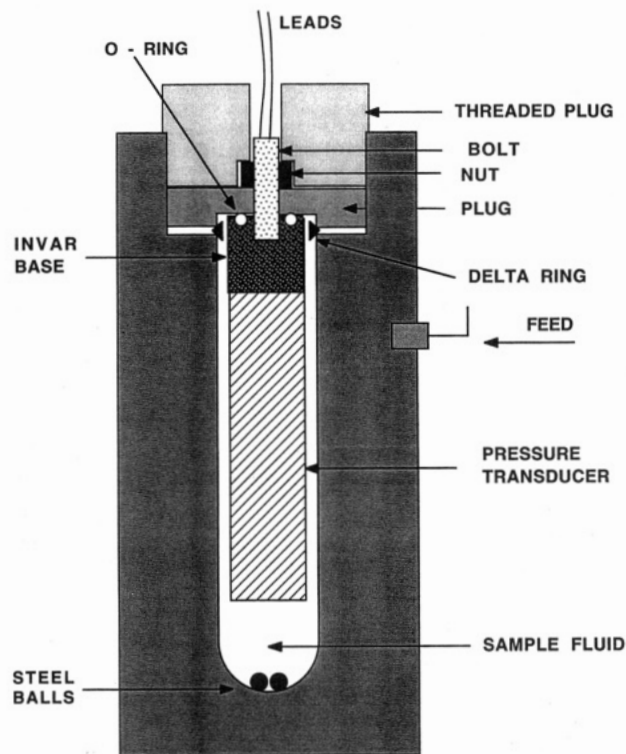
to a dead weight gauge (DH Instruments pneumatic dead weight gauge, model 50200), the vacuum system, the sample cylinder, and the vent line. All the components of this manifold are rated to 200 MPa. Stainless steel tubing (0.317 cm o.d.) is used for all the lines.

All of the data acquisition and temperature control is accomplished with a microcomputer equipped with an IEEE-488 interface. The signals from the different temperature sensors in the apparatus are selected by a digital scanner (Keithley, Inc., model 705) and measured with a digital nanovoltmeter (Keithley, Inc., model 181). The signal from the pressure sensor is measured with a digital frequency counter (Hewlett-Packard, model 5384A). Using a control algorithm, the computer generates control signals for the heaters which are sent to a multichannel digital to analog (D/A) converter. The signals from the D/A converter actuate the power supplies which drive the individual heaters of the system.

The control strategy used is initially ac heating at high power levels applied until the temperature is 1.0 K below the set point. Then, dc heating is applied at much lower power levels until the temperature is 50 mK below the set point. Finally, a proportional-integral (PI) control algorithm drives the temperature to ±2 mK from the set point. The temperature gradient of the cell is driven to ±2 mK.

The cell is designed to withstand a maximum pressure of 200 MPa with a safety factor of 2.5. The wall thickness has been sized according to ASME specifications (5). It is a cylindrical vessel with 2.738 cm i.d. and 7.937 cm o.d. and a total length of 17.15 cm. The transducer which fits in the cell is a cylinder with a 2.54 cm o.d. and 7.62 cm long. The internal length of the cell is 10.16 cm. The sample volume is approximately 13 cm^3.

Figure 2 is a schematic diagram of the cell, including the pressure transducer. This arrangement reduces the dead volume in the tubing connecting the sample cell to the pressure transducer.

A Be–Cu "Δ" ring seals the gap between the plug and the main body of the cell. A small pin prevents rotation of the plug when the threaded plug is tightened to make the
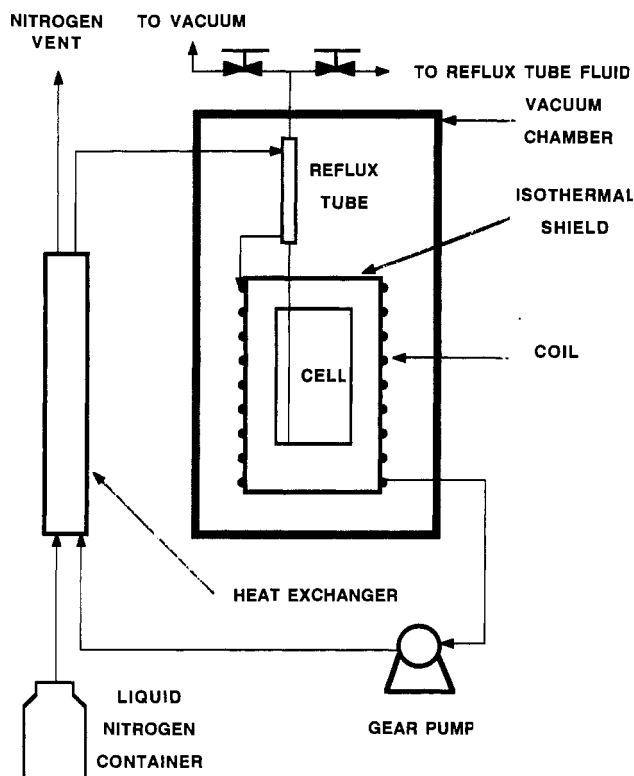
Figure 3. Schematic of the cooling system.

initial seal. This closure follows the design of Verbrugge *et al.* (*6*). A gold-plated, stainless steel O-ring seals the gap between the plug and the pressure transducer. The fitting for the feed port is cone and thread. The feed valve is on top of the sample cell to minimize the temperature gradient between the valve and tubing and the cell. The valve is of the same type as those used in the feed manifold. The sample is stirred by two steel balls inside the cell which are activated by a magnetic stirrer situated directly below the cell outside the apparatus.

The cooling system consists of a heat exchanger which cools liquid propane with liquid nitrogen, and the liquid propane cools the isothermal shield and the cell. Liquid nitrogen is not used directly as the cooling fluid because it provides unstable cooling due to the large temperature difference between the boiling point of nitrogen and the temperature of the apparatus.

The main components of the cooling system consist of a heat exchanger, a gear pump, a cooling coil for the isothermal shield, a reflux tube, and a liquid nitrogen container. Figure 3 presents a schematic diagram of the cooling system.

We selected propane as the cooling medium because of its low freezing point (85.5 K) and low viscosity (less than 1 mPa·s) at temperatures as low as 130 K. Also, propane has a reasonable vapor pressure (about 0.9 MPa) at room temperature.

The heat exchanger is a copper tube coil placed inside a shell made of a 3.81 cm o.d. pipe. The pipe is insulated with a 2.5 cm thick layer of a porous rubber material. The coil is 10 cm above the liquid nitrogen feed port to avoid the possibility of propane freezing. Liquid propane flows inside the coil while liquid nitrogen vaporizes inside the shell and exhausts to the atmosphere. The coil provides a heat exchange area of approximately 4000 cm². A closed container with a capacity of 0.15 m³ stores the liquid nitrogen which exerts a pressure of 0.2 MPa. This pressure is the driving force to force the nitrogen through the heat exchanger.

The liquid propane is pumped with a magnetic gear pump (Micropump, model 180). This pump can handle a system pressure drop of up to 0.3 MPa and a volumetric flow rate of 20 cm³·min⁻¹. Its maximum operating pressure is 4 MPa. The temperature range specified by the manufacturer is 200–410 K; however, we have used the pump at fluid temperatures as low as 170 K without problems. The pump is driven by a 0–24 V dc motor. The cooling power of the system can be controlled by regulating the volumetric flow rate of the gear pump.

The reflux tube cools the cell. The bottom section of the tube is in good thermal contact with the cell, and the top section of the tube forms a small double pipe heat exchanger. Cold propane flowing through the shell of this small heat exchanger causes the fluid inside the tube to condense. The condensed fluid falls to the bottom section of the tube where it evaporates, and the condensation–evaporation cycle inside the tube cools the cell. Cooling ceases upon evacuation of the reflux tube. In this system, ethane and propane are refrigerants for the reflux tube. The system has a cooling power of about 45 W and cools the apparatus at a rate of 0.5 K·min⁻¹.

Temperature was measured with a platinum resistance thermometer (MINCO, model XS9691) which has been calibrated against a platinum resistance temperature standard (Rosemount Inc., model 162CE, serial number 1437) whose calibration is traceable to the National Institute of Standards and Technology. The accuracy of this standard thermometer is 10 mK. The calibration covers a temperature range of 177–403 K with a precision of ±2 mK.

The pressure transducer (Transducer Technologies, Inc., model 3310) has been calibrated *in situ* against a primary pressure gauge (DH Instruments dead weight gauge, model 50200). The calibration covers pressures from 0 to 100 MPa at three temperatures: 215, 260, and 300 K. Along each isotherm, the calibration was made at increments of 10 MPa with increasing and decreasing pressures to check for hysteresis. Pressures measured with this transducer are precise to ±2 kPa, and the calibration equation is accurate to 10 kPa.

The volume of the cell changes with pressure and temperature according to

$$V/V_{ref} = 1 + \alpha(T - T_{ref}) + \beta(p - p_{ref}) \qquad (1)$$

so that for a given isomole ("isochore")

$$\varrho/\varrho_{ref} = (V/V_{ref})^{-1} = \{1 + \alpha(T - T_{ref}) + \beta(p - p_{ref})\}^{-1} \qquad (2)$$

In these equations, V is volume, T is temperature, p is pressure, α is the thermal distortion coefficient, β is the pressure distortion coefficient, ϱ is the molar density, and the subscript ref denotes reference conditions. The distortion coefficients were determined experimentally by measuring three isochores for methane at temperatures between 220 and 300 K and pressures from 20 to 75 MPa. Values of $\alpha = 1.6 \times 10^{-4}$ K⁻¹ and $\beta = 1.5 \times 10^{-4}$ MPa⁻¹ describe the methane calibration isochores with a root-mean-square deviation of 0.08%.

The densities of two of the $CO_2 + N_2$ mixtures were measured at 300 K with a pycnometer. The pycnometer consists of a sample cell suspended from an electronic balance surrounded by an isothermal copper shield in a helium gas bath. The sample mass in the cell is determined by weighing; the volume of the cell (approximately 10 cm³) is determined by calibration at several temperatures and pressures with degassed, deionized liquid water.

The balance (Arbor, model 507) has a resolution of ±0.1 mg and a capacity of 0.5 kg. The pressure is measured with a pressure transducer (Rosemount, model 1333G10) with an accuracy of ±0.01 MPa. The temperature is measured with a platinum resistance thermometer (MIN-CO, model S-1069). The thermometer is precise to ±0.001 K and accurate to ±0.01 K. Typical standard deviations for a series of 10 consecutive balance readings are 0.2–0.3 mg. The tare of the balance rarely changes by more than ±1 mg between the beginning and end of an isotherm. The overall error in the experimental densities (95% confidence) is

$$\delta \varrho/(kg \cdot m^{-3}) = [\{8 \times 10^{-4}\varrho/(kg \cdot m^{-3})\}^2 + (0.1)^2]\Omega \quad (3)$$

The mixtures were prepared gravimetrically using a Voland Corp. (model HCE25) double pan balance with a capacity of 25 kg and a resolution of 2.5 mg. The nitrogen, with a specified purity of better than 99.9995 mol %, was supplied by Air Products. The carbon dioxide was supplied by Scientific Gas Products with a specified purity of better than 99.996 mol %. The nitrogen was used without further purification. Dissolved air was removed from the pure carbon dioxide by alternately freezing and thawing the sample under vacuum.

Results

The following properties for CO_2 (1) + N_2 (2) were measured: fluid densities at 285 and 300 K at pressures from 10 to 70 MPa using the pycnometer, fluid densities over a temperature range of 205–300 K and a pressure range of 10–80 MPa using an isochoric apparatus, fluid–fluid equilibria over a temperature range of 207–268 K and a pressure range of 10.8–21.5 MPa using another isochoric apparatus (7), and solid–fluid phase boundaries through isochoric experiments (qualitative information only).

Isothermal Densities. Densities measured with the pycnometer at $x_1 = 0.5037$ at temperatures of 285 and 300 K and pressures to 70 MPa and at $x_1 = 0.3991$ at $T = 300$ K and pressures to 70 MPa are given in Table 1. These results were used to determine the parameters a_i in

$$\varrho = \sum a_i p^i \quad (4)$$

for each isotherm, for use in calculating base densities for isochores.

Isochoric Densities. Nineteen isochores were measured at $x_1 = 0.5037$ over a temperature range of 205–300 K at pressures between 8 and 78 MPa (a total of about 190 experiments). The base density for one isochore (isochore 7) was determined from the isothermal densities at 285 K, and the base densities for the other isochores were determined from the isothermal densities at 300 K. Table 2 gives the measured temperatures and pressures, as well as the densities calculated using eqs 2 and 4, for each isochore.

For $x_1 = 0.3991$, six isochores over a temperature range of 207–300 K at pressures from 8 to 80 MPa were measured. Table 3 gives the measured temperatures and pressures, as well as the densities calculated using eq 4 fit to pycnometer results at 300 K and eq 2.

Three isochores were measured for $x_1 = 0.4459$ at temperatures from 207 to 300 K at pressures between 17 and 64 MPa. Table 4 contains the measured pressures and temperatures and calculated densities for each isochore. No pycnometer measurements were made for this composition, so the base densities were calculated using an equation of state. The chosen equation, DDMIX (8), described the 300 K isotherms for $x_1 = 0.3991$ and $x_1 = $

Table 1. Experimental Isothermal Densities (Pycnometer) for CO_2 (1) + N_2 (2)^a

T/K	p/MPa	ϱ/(mol· m^{-3})	T/K	p/MPa	ϱ/(mol· m^{-3})
		$x_1 = 0.3991$			
300.000	69.031	19 843	300.000	48.387	17 305
300.000	65.422	19 495	300.000	43.634	16 498
300.000	62.028	19 128	300.000	39.295	15 654
300.000	58.630	18 731	300.000	34.539	14 578
300.000	55.214	18 291	300.000	30.092	13 780
300.000	51.775	17 816			
		$x_1 = 0.5037$			
285.000	69.189	21 561	300.000	69.028	20 667
285.000	57.633	20 450	300.000	58.681	19 607
285.000	48.491	19 343	300.000	50.230	18 541
285.000	41.194	18 238	300.000	43.426	17 488
285.000	35.359	17 137	300.000	37.763	16 425
285.000	30.659	16 028	300.000	33.118	15 368
285.000	26.842	14 917	300.000	29.248	14 302
285.000	23.732	13 814	300.000	26.056	13 259
285.000	21.142	12 705	300.000	23.267	12 195
285.000	18.932	11 599	300.000	20.829	11 123
285.000	16.990	10 479	300.000	18.707	10 069
285.000	15.270	9 375	300.000	16.744	9 007
285.000	13.678	8 273	300.000	14.914	7 942
285.000	12.150	7 173	300.000	13.165	6 888
285.000	10.616	6 055	300.000	11.413	5 818
285.000	9.050	4 948	300.000	9.643	4 758
285.000	7.376	3 837	300.000	7.789	3 695
285.000	5.543	2 732	300.000	5.819	2 645
285.000	3.502	1 627	300.000	3.652	1 579
285.000	1.192	522	300.000	1.262	516

^{a} The molar densities were calculated from the observed mass densities using the molar masses: $M(CO_2) = 44.0098$ and $M(N_2) = 28.01348$. The accuracies of the measured densities are described by eq 3 in the text.

0.5037 with systematic deviations ranging from 0.35% to 0.40% over the pressure range of interest. The base densities for $x_1 = 0.4459$ were calculated by assuming that the systematic deviation for that composition could be described by a linear interpolation between the deviations at a given pressure for the 0.3991 and 0.5037 compositions. The density calculated from the equation of state was then adjusted by the interpolated systematic deviation. The base densities calculated using this procedure are estimated to be accurate to ±0.2%.

Fluid–Fluid Equilibria. A phase boundary is located by observing the discontinuous change in slope of an isochore. To determine this condition, we fit the single phase isochoric pressures with a polynomial of order 1 in temperature and the two phase isochoric data with a polynomial of order 1 or 2 in temperature. The intersection of these two functions is the phase boundary. This discontinuous change in the slope of an isochore is difficult to locate near the cricondentherm (local temperature maximum in a p, T phase diagram) because the slope of an isochore for a binary mixture is continuous at the cricondentherm (9, 10).

For $x_1 = 0.5037$, we determined 14 phase boundary points. The phase boundary for one isochore could not be located because we measured only one point in the two phase region. Also, we could not determine the phase boundaries of four other isochores because they cross the fluid–fluid phase boundary close to the cricondentherm. We determined six phase boundary locations for the mixture with $x_1 = 0.3991$ and three for $x_1 = 0.4457$. The phase boundary conditions (T, p, ϱ) are given in Table 5 for each composition. Figure 4 compares the present results with those of Esper *et al.* (12). All the isopleths become nearly identical at about 16 MPa.

Table 2. Measured Temperatures and Pressures and Calculated Densities along Isochores for CO_2 (1) + N_2 (2) with $x_1 = 0.5037$[a]

T/K	p/MPa	ρ/(mol·m⁻³)	φ	T/K	p/MPa	ρ/(mol·m⁻³)	φ	T/K	p/MPa	ρ/(mol·m⁻³)	φ	T/K	p/MPa	ρ/(mol·m⁻³)	φ
								Isochore 1							
300.004	77.527	21 535	1	284.791	68.541	21 617	1	219.584	27.836	21 981	1	208.278	21.394	22 044	2
297.076	75.821	21 550	1	223.101	30.002	21 962	1	217.184	26.391	21 995	1	207.648	21.374	22 046	2
296.294	75.357	21 555	1	221.270	28.879	21 972	1	214.579	24.852	22 010	1	207.247	21.359	22 048	2
287.174	69.940	21 604	1												
								Isochore 2							
300.009	64.250	20 225	1	220.827	21.762	20 618	1	217.969	20.417	20 632	1	213.481	19.294	20 651	2
299.904	64.199	20 226	1	220.052	21.392	20 622	1	216.022	19.597	20 641	1	212.806	19.252	20 653	2
299.795	64.143	20 226	1	218.950	20.867	20 627	1	214.394	19.347	20 647	2	212.058	19.211	20 656	2
								Isochore 3							
300.056	53.897	19 020	1	228.693	19.890	19 339	1	224.820	18.366	19 356	1	222.425	18.028	19 365	2
299.997	53.873	19 020	1	227.070	19.227	19 346	1	223.077	18.077	19 362	2	222.025	18.008	19 366	2
299.895	53.825	19 021	1	225.942	18.781	19 351	1								
								Isochore 4							
299.997	45.893	17 894	1	239.602	20.271	18 139	1	235.573	18.710	18 155	1	229.637	17.102	18 177	2
299.941	45.867	17 894	1	238.342	19.777	18 144	1	234.156	18.193	18 161	1	228.955	17.060	18 179	2
299.852	45.827	17 895	1	237.158	19.313	18 149	1	230.101	17.136	18 176	2				
								Isochore 5							
300.139	39.770	16 817	1	245.534	19.174	17 018	1	242.066	17.976	17 031	1	236.834	16.448	17 049	1
300.007	39.715	16 817	1	244.825	18.924	17 020	1	239.957	17.270	17 038	1	236.260	16.376	17 051	2
299.860	39.661	16 818	1	244.098	18.669	17 023	1								
								Isochore 6							
300.045	34.863	15 782	1	245.856	16.833	15 963	1	242.893	16.022	15 973	1	240.509	15.747	15 980	2
299.999	34.846	15 782	1	245.341	16.685	15 965	1	241.493	15.802	15 977	2	239.646	15.695	15 982	2
299.881	34.803	15 782	1	244.081	16.332	15 969	1								
								Isochore 7							
300.015	31.002	14 808	1	250.292	16.203	14 961	1	247.353	15.460	14 969	1	244.094	15.126	14 978	2
299.819	30.942	14 809	1	249.582	16.014	14 963	1	246.887	15.362	14 971	1	243.394	15.085	14 980	2
299.742	30.912	14 809	1	248.353	15.697	14 966	1	245.220	15.200	14 975	2				
								Isochore 8							
300.004	27.915	13 891	1	297.037	27.150	13 899	1	252.969	15.334	14 023	1	248.739	14.650	14 034	2
299.854	27.896	13 891	1	254.599	15.722	14 018	1	251.684	15.025	14 026	1	248.104	14.608	14 035	2
299.735	27.864	13 892	1	253.649	15.494	14 021	1	249.312	14.691	14 033	2				
								Isochore 9							
300.051	25.515	13 059	1	297.076	24.756	13 066	1	254.354	14.536	13 177	1	251.170	14.196	13 184	2
299.947	25.467	13 059	1	259.402	15.646	13 164	1	252.143	14.268	13 182	2	250.288	14.127	13 186	2
299.812	25.458	13 059	1	258.207	15.375	13 167	1								
								Isochore 10							
300.025	23.495	12 281	1	261.445	14.909	12 374	1	258.319	14.272	12 381	1	254.393	13.749	12 390	2
299.938	23.470	12 282	1	260.851	14.790	12 375	1	254.878	13.788	12 389	2	253.515	13.684	12 392	2
299.815	23.443	12 282	1	260.100	14.632	12 377	1								
								Isochore 11							
300.036	21.740	11 531	1	262.002	14.023	11 615	1	259.022	13.472	11 622	2	255.876	13.210	11 628	2
299.878	21.707	11 531	1	261.369	13.903	11 617	1	256.520	13.263	11 627	2	255.163	13.148	11 630	2
299.771	21.679	11 532	1	260.633	13.758	11 618	1								
								Isochore 12							
300.047	20.232	10 827	1	267.952	14.293	10 892	1	263.822	13.536	10 901	1	258.599	12.852	10 911	2
299.841	20.191	10 827	1	267.440	14.203	10 893	1	259.244	12.908	10 910	2	257.601	12.758	10 913	2
299.732	20.162	10 827	1	266.759	14.078	10 895	1								
								Isochore 13							
300.040	17.975	9680	1	270.077	13.225	9733	1	266.636	12.667	9739	1	260.443	11.957	9750	2
299.865	17.948	9680	1	269.332	13.110	9734	1	261.294	12.035	9749	2	259.640	11.875	9751	2
299.713	17.926	9680	1	268.387	12.947	9736	1								
								Isochore 14							
300.079	16.160	8673	1	273.444	12.524	8715	1	269.175	11.927	8722	1	264.596	11.383	8729	2
299.841	16.137	8674	1	272.536	12.394	8717	1	265.440	11.466	8728	2	263.772	11.303	8730	2
299.727	16.118	8674	1	271.885	12.304	8718	1								
								Isochore 15							
300.035	14.545	7730	1	272.787	11.377	7768	1	269.957	11.030	7772	1	264.780	10.479	7779	2
299.866	14.528	7730	1	272.065	11.291	7769	1	266.004	10.599	7777	2	263.368	10.341	7781	2
299.741	14.507	7731	1	271.068	11.172	7770	1								
								Isochore 16							
300.074	13.215	6918	1	299.703	13.176	6919	1	272.143	10.428	6952	1	266.717	9.866	6959	2
299.853	13.196	6919	1	273.127	10.524	6951	1	270.790	10.286	6954	1	265.817	9.777	6960	2
								Isochore 17							
300.094	11.205	5685	1	272.886	9.358	5712	1	269.586	9.122	5715	1	263.880	8.713	5721	2
299.893	11.185	5685	1	271.616	9.270	5713	1	265.080	8.804	5719	2	262.794	8.630	5722	2
299.795	11.178	5686	1	270.196	9.168	5714	1								

Table 2 (Continued)

T/K	p/MPa	$\varrho/(mol \cdot m^{-3})$	ϕ	T/K	p/MPa	$\varrho/(mol \cdot m^{-3})$	ϕ	T/K	p/MPa	$\varrho/(mol \cdot m^{-3})$	ϕ	T/K	p/MPa	$\varrho/(mol \cdot m^{-3})$	ϕ
							Isoch	ore 18							
300.022	9.582	4724	1	273.439	8.194	4745	1	264.385	7.686	4752	1	256.448	7.146	4759	2
299.979	9.580	4724	1	271.689	8.105	4746	1	261.311	7.530	4755	1	255.792	7.093	4759	2
299.918	9.575	4724	1	270.094	8.017	4747	1	257.939	7.268	4757	2				
							Isoch	ore 19							
300.057	10.116	5034	1	269.971	8.389	5059	1	264.915	8.073	5064	1	259.492	7.708	5068	2
299.873	10.100	5034	1	269.444	8.361	5060	1	260.585	7.799	5067	2	258.885	7.657	5069	2
299.701	10.085	5034	1	268.409	8.291	5061	1								

^{a} The calculated densities are accurate to ±0.2% above 250 K and to ±0.3% below 250 K. ϕ denotes the number of phases present.

Table 3. Measured Temperatures and Pressures and Calculated Densities along Isochores for CO_2 (1) + N_2 (2) with $x_1 = 0.3991^a$

T/K	p/MPa	$\varrho/(mol \cdot m^{-3})$	ϕ	T/K	p/MPa	$\varrho/(mol \cdot m^{-3})$	ϕ
			Isochore 1				
300.084	65.012	19 448	1	212.275	22.306	19 854	1
299.992	64.963	19 448	1	210.275	21.741	19 862	1
299.844	64.901	19 449	1	208.674	21.156	19 869	2
215.627	23.816	19 839	1	207.654	21.090	19 873	2
213.503	22.856	19 848	1	207.001	21.041	19 875	2
			Isochore 2				
300.194	55.689	18 344	1	221.831	22.133	18 672	1
300.088	55.644	18 345	1	218.355	20.761	18 687	1
300.035	55.623	18 345	1	214.377	19.696	18 702	2
225.550	23.670	18 657	1	213.463	19.627	18 705	2
224.013	23.037	18 663	1	212.591	19.565	18 708	2
			Isochore 3				
300.161	42.539	16 287	1	231.641	19.487	16 525	1
300.070	42.507	16 287	1	228.774	18.595	16 535	1
299.982	42.484	16 287	1	225.043	17.760	16 547	2
235.924	20.884	16 510	1	224.334	17.706	16 549	2
233.995	20.251	16 517	1	223.481	17.641	16 552	2
			Isochore 4				
300.041	37.796	15 332	1	234.196	18.072	15 542	1
299.955	37.770	15 332	1	232.152	17.509	15 548	1
299.870	37.748	15 332	1	229.474	17.031	15 556	2
236.155	18.629	15 535	1	228.575	16.959	15 558	2
235.214	18.357	15 538	1	227.498	16.879	15 561	2
			Isochore 5				
300.095	33.976	14 429	1	237.992	17.261	14 611	1
299.999	33.953	14 429	1	233.659	16.370	14 623	2
299.806	33.897	14 430	1	232.495	16.273	14 626	2
242.815	18.525	14 597	1	231.720	16.210	14 628	2
240.217	17.837	14 604	1				
			Isochore 6				
300.270	30.842	13 577	1	241.986	16.725	13 734	1
300.167	30.815	13 578	1	237.427	15.799	13 747	2
300.066	30.794	13 578	1	236.250	15.697	13 749	2
249.296	18.473	13 715	1	235.489	15.625	13 751	2
245.956	17.678	13 724	1				

^{a} The calculated densities are accurate to ±0.2% above 250 K and to ±0.3% below 250 K. ϕ denotes the number of phases present.

Table 4. Measured Temperatures and Pressures and Calculated Densities along Isochores for CO_2 (1) + N_2 (2) with $x_1 = 0.4459^a$

T/K	p/MPa	$\varrho/(mol \cdot m^{-3})$	ϕ	T/K	p/MPa	$\varrho/(mol \cdot m^{-3})$	ϕ
			Isochore 1				
300.012	52.108	18 190	1	240.166	26.629	18 437	1
299.983	52.074	18 190	1	235.278	24.545	18 457	1
289.089	47.591	18 234	1	230.042	22.372	18 479	1
279.689	43.649	18 273	1	220.293	18.818	18 519	2
269.860	39.456	18 313	1	216.891	18.600	18 530	2
263.543	36.734	18 339	1	214.069	18.441	18 539	2
249.850	30.797	18 396	1				
			Isochore 2				
300.025	64.335	19 639	1	231.758	29.411	19 962	1
299.998	64.323	19 639	1	222.010	24.455	20 008	1
280.200	54.536	19 731	1	208.974	20.182	20 064	2
256.000	42.091	19 845	1	207.102	20.024	20 071	2
			Isochore 3				
300.009	47.386	17 507	1	227.030	18.581	17 792	1
297.070	46.311	17 518	1	225.846	18.226	17 796	1
296.251	45.996	17 521	1	224.285	18.032	17 801	2
295.020	45.524	17 526	1	223.124	17.971	17 805	2
228.901	19.207	17 785	1	221.938	17.900	17 808	2
227.939	18.885	17 788	1				

^{a} The calculated densities are accurate to ±0.2% above 250 K and to ±0.3% below 250 K. ϕ denotes the number of phases present.

Table 5. Phase Boundary Conditions for CO_2 (1) + N_2 (2)^a

T/K	p/MPa	$\varrho/(mol \cdot m^{-3})$	T/K	p/MPa	$\varrho/(mol \cdot m^{-3})$
		$x_1 = 0.3991$			
210.095	21.254	19 864	230.785	17.130	15 553
216.264	19.833	18 696	235.038	16.485	14 620
226.753	17.891	16 542	238.532	15.899	13 744
		$x_1 = 0.4459$			
214.188	20.624	20 046	225.488	18.101	17 797
221.551	18.891	18 515			
		$x_1 = 0.5037$			
208.929	21.416	22 042	253.563	14.376	13 179
215.579	19.417	20 643	256.581	13.916	12 385
224.234	18.153	19 359	259.245	13.492	11 621
231.416	17.220	18 172	261.559	13.121	10 906
242.167	15.842	15 976	264.922	12.387	9 743
246.524	15.282	14 971	266.953	11.614	8 725
250.677	14.578	14 030	268.039	10.798	7 774

^{a} The temperatures and pressures are accurate to ±0.1% and the densities to ±0.3% below 250 K and ±0.2% above 250 K.

Fluid—Solid Equilibria. The onset of solid formation was observed in these mixtures. Because supercooling appeared to be significant and we could not mix the samples well when solids were present, these observations are only qualitative. However, they are interesting because a temperature range exists for which the isochores have negative slopes. Figure 5 depicts qualitatively the phase behavior at fixed overall composition of a $N_2 + CO_2$ mixture for compositions in the range of those studied in this work. The dashed line is the prediction of Hall and Kreglewski (11) for the fluid—fluid saturation boundary in the absence of solid formation. At certain conditions a solid phase forms, which we believe to be essentially pure carbon dioxide. So, as the mixture cools below the solid/fluid phase boundary, the fluid phase(s) is rapidly depleted of carbon dioxide by the condensing solid. As a result, the composition of the fluid phase varies rapidly with temperature in the shaded region. To the left of the shaded region, the mixture exists as an essentially pure nitrogen fluid phase in equilibrium with an essentially pure CO_2 solid. Figure 5 also shows two typical isochores. As the mixture cools
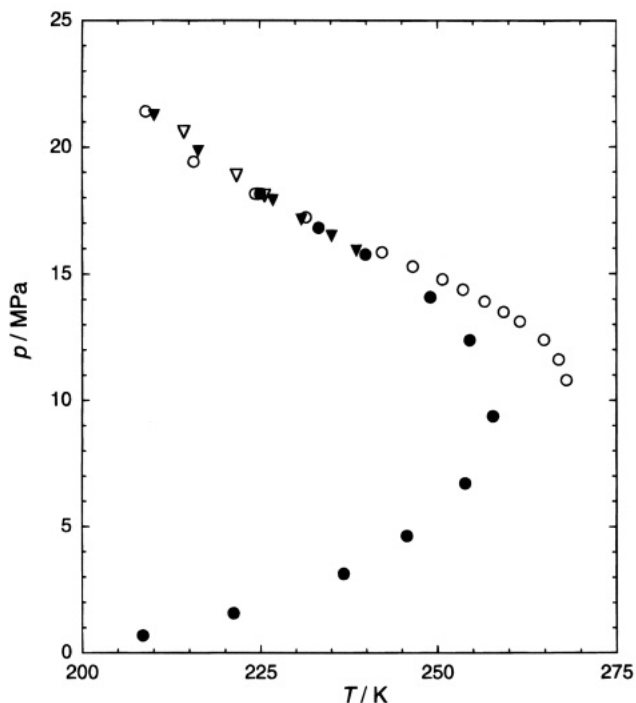
Figure 4. Experimental phase boundaries for CO_2 (1) + N_2 (2). The symbols denote various mole fractions: this work, $\bigcirc$, $x_1 = 0.5037$; $\triangledown$, $x_1 = 0.4459$; $\blacktriangledown$, $x_1 = 0.3991$; Esper *et al.* (*11*), $\bullet$, $x_1 = 0.4470$.
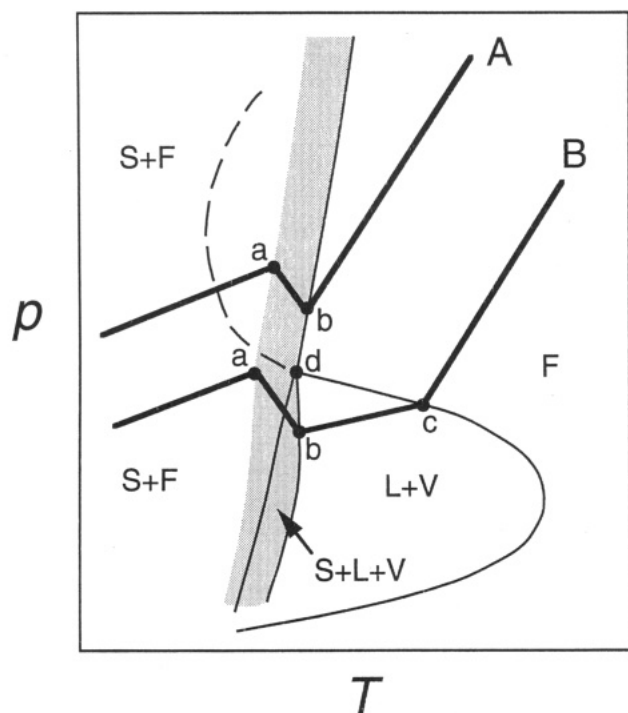

Figure 5. Qualitative isochoric behavior illustrating liquid + vapor and solid + vapor equilibria for CO_2 (1) + N_2 (2). The shaded region is the CO_2 depletion zone. F denotes a fluid phase.

along isochore A, a frost point occurs at b, and the mixture changes from a single phase fluid to a solid + fluid two phase equilibrium. Upon cooling along isochore B, a dew point occurs at c and then the solid condenses at b so that a three phase solid + liquid + vapor equilibrium occurs over a narrow range of temperature. Point d is the intersection of the phase boundary between a single phase fluid and solid + fluid equilibrium, with the phase boundary between a single phase and vapor + liquid equilibrium. Point d is most likely not a critical point.

It is the rapid depletion of carbon dioxide in the fluid phase which leads to the negative slope of the isochore between a and b on each isochore. If the fluid approximately obeys the principle of corresponding states, the equation of state in reduced variables has a universal form, $p_r = f(\varrho_r, T_r)$, where both $(\partial p_r/\partial \varrho_r)_T$ and $(\partial p_r/\partial T_r)_\varrho$ are always positive. However, it is possible for T_r ($=T/T_c$) to increase while T decreases if the mixture critical temperature decreases sufficiently rapidly with decreasing temperature because of the rapid depletion of carbon dioxide in the liquid phase.

Discussion

Kreglewski and Hall (*11*) estimated the phase behavior of CO_2 (1) + N_2 (2) mixtures for pressures to 300 MPa using the BACK EOS. For a range of x_1 between 0.42 and 0.58, the equation predicts an open isopleth with gas + gas equilibria at high pressures. Our results corroborate the open isopleth behavior. The results also indicate that, at a higher pressure, a solid + gas instead of a gas + gas phase boundary exists (the calculations do not predict a solid phase because the equation of state is valid only for fluids). The solid + gas boundary appears at about (204.5 ± 1.5) K over a pressure range of 8−21 MPa. We did not measure the solid + gas phase boundary at higher pressures. In addition, we did not detect a significant difference in the temperature at which the solid first appears among the three compositions at the higher pressures. We have found no measurements in the literature with which to compare these results. Our results indicate an open isopleth and no critical point for the CO_2 + N_2 mixtures measured in this work. The upper saturation pressure increases monotonically as the temperature decreases until the isopleth is intersected by the solid + gas phase boundary.

Esper *et al.* (*12*) determined phase equilibria for CO_2 (1) + N_2 (2) with $x_1 = 0.4470$ in a Burnett isochoric experiment. Our lowest pressure and the highest pressure from Esper agree within the combined uncertainties of the pressure measurements and the minor differences in composition.

Several researchers (*13−18*) have published vapor-liquid equilibrium (VLE) measurements for CO_2 + N_2. The different natures of these data and our data preclude direct comparisons. No VLE measurements exist for temperatures below 218 K or for pressures above 18.5 MPa. Our measurements provide phase boundary measurements for pressures up to 21.4 MPa and temperatures as low as 209 K. We know of no other experimental densities for this system covering the temperature and pressure ranges studied in this work.

Literature Cited

(1) Michels, A.; Wassenaar, T.; Zwietering, Th. N. *Physica* **1952**, *18*, 67.
(2) Vennix, A. J.; Leland, T. W.; Kobayashi, R. *Adv. Cryog. Eng.* **1966**, *12*, 700.
(3) Duarte-Garza, H. A. A high pressure isochoric apparatus to determine accurate *PVT* and phase equilibria on fluids: applications to CO_2+N_2. Ph.D. Dissertation, Texas A&M University, College Station, TX, 1988.
(4) Lau, R. A. A continuously weighed pycnometer providing densities for carbon dioxide + ethane mixtures between 240 and 350 K at pressures up to 35 MPa. Ph.D. Dissertation, Texas A&M University, College Station, TX, 1986.
(5) Anon. *ASME Boiler and Pressure Vessel Code;* ASME: New York, 1977.
(6) Verbrugge, R.; Schouten, J. A.; Trappeniers, N. J. *Rev. Sci. Instrum.* **1985**, *56*, 625.
(7) Yurttas, L.; Holste, J. C.; Hall, K. R.; Gammon, B. E.; Marsh, K. N. *J. Chem. Eng. Data* **1994**, *39*, 418.
(8) Ely, J. F. NIST Mixture Property program (DDMIX) Version 9.07, National Institute of Standards and Technology, Office of Standard Reference Data.

(9) Dorion, T.; Behringer, R. P.; Meyer, H. *J. Low Temp. Phys.* **1976**, *24*, 345.

(10) Rowlinson, J. S.; Esper, G. J.; Holste, J. C.; Hall, K. R.; Barrufet, M. A.; Eubank, P. T. *Equations of State Theory and Applications;* ACS Symposium Series; American Chemical Society: Washington, DC, 1986.

(11) Kreglewski, A.; Hall, K. R. *Fluid Phase Equilib.* **1983**, *15*, 11.

(12) Esper, G. J.; Bailey, D. M.; Holste, J. C.; Hall, K. R. *Fluid Phase Equilib.* **1989**, *49*, 35.

(13) Zenner, G. H.; Dana, L. I. *Am. Inst. Chem. Eng. Symp. Ser.* **1963**, *59*, 36.

(14) Muirbrook, A.; Prausnitz, J. M. *AIChE J.* **1965**, *11*, 1092.

(15) Arai, Y.; Kaminishi G.; Saito, S. *J. Chem. Eng. Jpn.* **1971**, *4*, 113.

(16) Somait, F. A.; Kidnay, A. J. *J. Chem. Eng. Data* **1978**, *23*, 301.

(17) Dorau, W.; Al-Wakeel, M.; Knapp, H. *Cryogenics* **1983**, *11*, 29.

(18) Brown, T. S.; Sloan, E. D.; Kidnay, A. J. *Fluid Phase Equilib.* **1989**, *51*, 299.